In-situ EMI Measurements Using a Vibrating Intrinsic Reverberation Chamber

Frank B.J. Leferink[*+], Dick J. Groot Boerle[*], Fons A.G. Sogtoen[*],
Geert H.L.M Heideman[+], Wim C. van Etten[+]

[*] Thales Naval Systems
Hengelo, The Netherlands
leferink@signaal.nl

[+] University of Twente
Enschede, The Netherlands
leferink@cs.utwente.nl

Abstract: A new reverberation chamber with varying angles between wall, floor and ceiling and with vibrating walls is used for in-situ testing of a large radar antenna system. Inside this Vibrating Intrinsic Reverberation Chamber (VIRC) a diffuse, statistically uniform electromagnetic field is created without the use of a mechanical, rotating, mode stirrer. This chamber results in a better homogeneity and increased field strength compared to conventional mode stirred reverberation chambers. The experience gained with this VIRC and results obtained using the VIRC for in-situ electromagnetic interference (EMI) testing will be discussed.

1. Introduction

A reverberation chamber generally consists of a rectangular test room with metal walls and a mode stirrer, usually in the form of a large paddle, near the ceiling of the chamber. The equipment under test (EUT) is placed in the chamber and exposed to an electromagnetic field while the stirrer slowly revolves. The average response of the EUT to the field is found by integrating the response over the time period of one revolution of the stirrer. The metal walls of the chamber allow a large field to be built up inside the chamber. The EUT is therefore exposed to a high field level consisting of several different polarizations [1,2,3,4].
It has been shown [5, 6, 9, 10, 11, 12, 13, 14] that the variation of the boundary conditions deviate the resonant behaviour of a reverberation room. For proper mode separation we need asymmetric structures. On the other hand, circular structures result in focussing of rays and thus degrade the spatial uniformity. Wall irregularities and wall-floor angle irregularities show that the spatial uniformity and isotropicity can be improved.
By changing all angles of the wall-floor-ceiling of a reverberation room in a high velocity compared to the classic mode stirrer in mode stirred reverberation chambers we can use all beneficial effects. This technique is called Vibrating Intrinsic Reverberation Chamber (VIRC) and drawn schematically in Figure 1.
The VIRC is a reverberation chamber where the walls are made of flexible conducting material. It is mounted in a rigid structure and connected to that structure via flexible rubber strings, as shown in Figure 2.

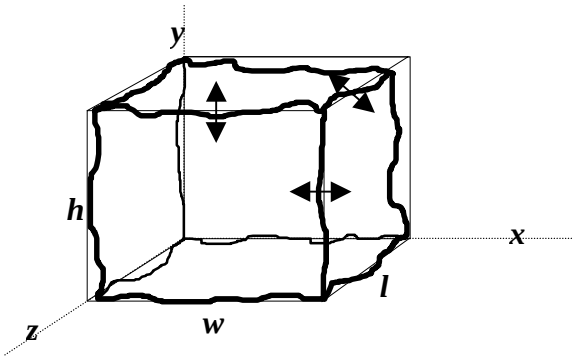

Figure 1: The VIRC: a flexible tent with irregularly shaped walls. The field is stirred by moving the walls

Figure 2: The VIRC hanging in strings

By moving one or more ridges or one or more walls the modal structure inside the chamber is changed. Because the frequency shift is much larger compared to what is possible with a conventional mode stirrer, the frequency range of the chamber is extended to lower frequencies compared to conventional (mode stirred) reverberation chambers with equal dimensions. Note the natural corrugation of the flexible walls in Figure 2 which is beneficial for the spatial uniformity too. Another advantage is that the flexible chamber can be erected inside a standard anechoic chamber where the EUT has been installed for standard EMI tests. Furthermore the VIRC

does not need extra space inside the laboratory: it can be folded and put away fast. The most important advantage of the flexible structure of the VIRC is that it can be installed in-situ.
The technique has been described in [16, 17, 18 and 19]. In this paper experience gained in practice, related to radiated emission and susceptibility EMI testing, will be discussed.

2. Visualisation of the spatial uniformity

In the prototype VIRC three fluorescent tubes are fixed in three orthogonal directions [15]. A field in the VIRC is generated by means of a generator tuned at approximately 3 GHz and an amplifier with an output level of 50 W. Due to the fields inside the VIRC the lights are glowing; bright at the point with a high field strength and dimmed at places with low field strength, as shown in Figure 3. The difference in intensity can be seen in more detail in Figure 4. By moving the VIRC the field structure is changed. This results in the time-averaged constant light intensity as shown in Figure 5.

Figure 3: Three fluorescent tube lights in the VIRC, at 3 GHz and 50 W injected power.

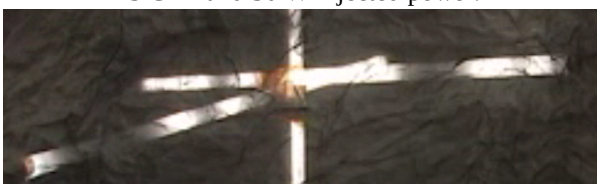

Figure 4: Detail of Figure 3. Note the difference in light intensity ~> field intensity.

Figure 5: Due to the vibration of the walls the light intensity is constant over the volume of the VIRC.

3. Experimental characterisation of a reverberation chamber

Numerous experiments could be carried out to characterize a reverberation chamber. Some of them are:

- Resonance frequency variation (Δf)
- Voltage Standing Wave Ratio (VSWR)
- Stirring Ratio (SR)
- (Angular) Correlation coefficient (ρ)
- Power Density Function (PDF)
- Cumulative Density Function (CDF)
- Spatial Field Uniformity (SFU)
- Chamber gain (CG)
- Quality Factor (Q)

Measurements have been carried out in a conventional mode stirred chamber and the first (prototype) VIRC. Results of the Δf, VSWR, SR, PDF and CDF have been presented in [16, 17, 18].
This paper is dedicated to the use of a VIRC which has been designed and built for in-situ radiated EMI testing of a large active phased array antenna. Numerous measurements have been carried out, and a selection has been presented in this paper. This includes stirring ratio, correlation coefficient, probability (and cumulative) density function and chamber gain measurements

4. In-situ testing using a VIRC

A VIRC has been designed and built for in-situ testing of an active phased array antenna. A picture of this VIRC is shown in Figure 6 and 7. The dimensions of this VIRC are 5x3x3m, resulting in a first resonance frequency of 58 MHz. The VIRC was fabricated by a tent manufacturer from the basic material we supplied. The walls were made from metalised (copper) fabric. The seams were overlapping, using double stitch. The interface with the EUT was made via a circumferencial galvanic connection, as shown in Figure 7.

Figure 6: The VIRC as built for in-situ testing

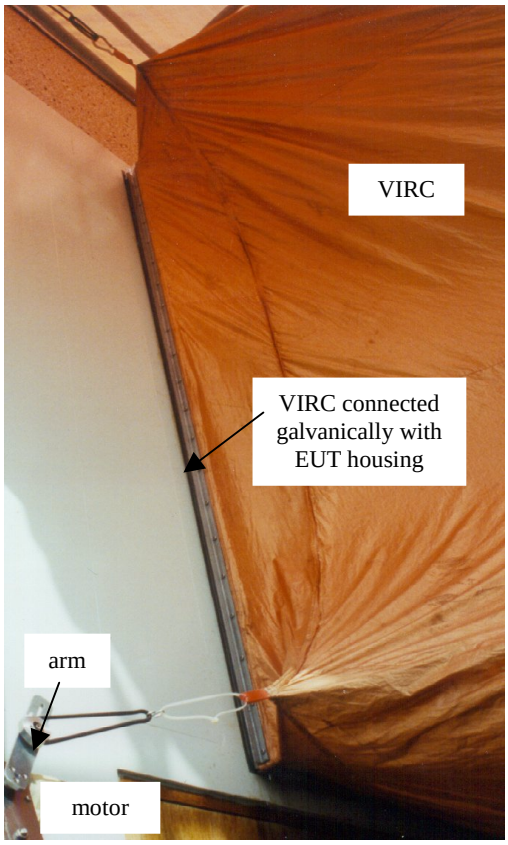

Figure 7: Interface with the EUT, and the excentric part inducing the vibration

All cable feedthroughs are either a waveguide-beyond-cutoff penetration for non-conducting parts, or a circumferencial galvanic connection for all conducting parts, such as cables. The vibration has been created by using automobile wiper motors with an excentric arm which is connected to the VIRC by means of an elastic rope, as shown in Figure 7.

5. VIRC validation

The VIRC has been validated before actual EMI test were performed. The EUT was not mounted in the VIRC during these measurements. Due to the limited length of a paper, only the most important test results at only a few frequencies are presented.

5.1. Stirring ratio

The stirring ratio indicates the effectiveness of a stirring mechanism. If the stirring ratio would be small then the boundary conditions are changed only slightly, and, as a result, the spatial uniformity could be low. In [12] a stirring ratio of at least 20 dB is considered as sufficient. The electric field strength in the three orthogonal directions was measured inside the VIRC while the boundary conditions were changing; i.e. the VIRC was vibrating. The movements were pseudo-random, by 8 motors with different rotation speed, creating a wall deviation of at least 10%. An electromagnetic field was generated inside the VIRC by an antenna. A generator activated the antenna. The field strength inside the VIRC has been measured using the Thomson-CSF ET2003 three-dimensional E-field sensor. The output signal of the sensor was fed to the optical receiver via an optical fiber. The output of the receiver was detected using a set of 5 logarithmic detectors. The detector makes use of an AD 8313 integrated circuit, which has a bandwidth of 2.5 GHz, a dynamic range of 70 dB, an amplitude flatness of ±1 dB, a noise level of less than –73 dBm and a response time of >40 ns. The DC level output, representing the field strength amplitude, was recorded by a sampling recorder AR1100. The data were saved and evaluated on a PC using Excel. The test set-up was as drawn in Figure 8.

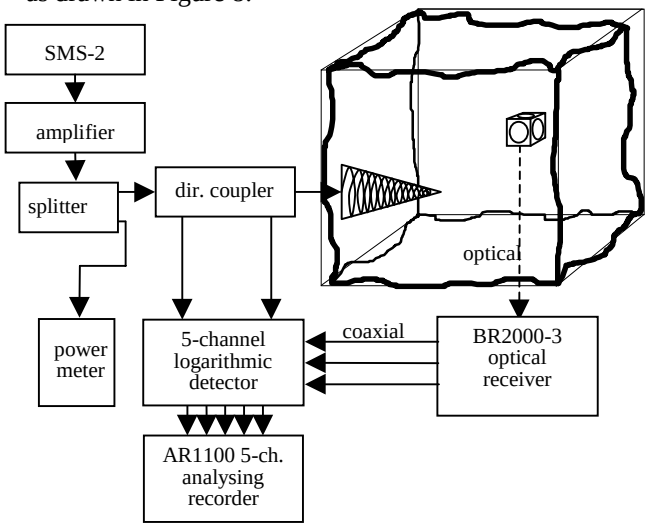

Figure 8: Test set-up for measuring the field strength inside the VIRC as function of change in boundary conditions

Measurements were performed at 25, 50, 75, 100, 150, 200, 250, 300, 400, 500, 600, 700, 800 and 900 MHz, and 1, 1.25, 1.5, 1.75, 2, 2.25, 2.5, 2.75 and 3 GHz. For every frequency 4000 samples have been taken with a sample time of 1 ms. The samples were recorded simultaneously for the incident and reflected power and the field strength for every axis, giving a total of 5 channels with 4000 samples.

The stirring ratio, or the field strength as function of the time, for 100 MHz and 1 GHz has been drawn in Figures 9 and 10 respectively. It can be observed in the figures that the SR for 100 MHz and 1000 MHz satisfies the rule SR>20dB, as stated in [12].

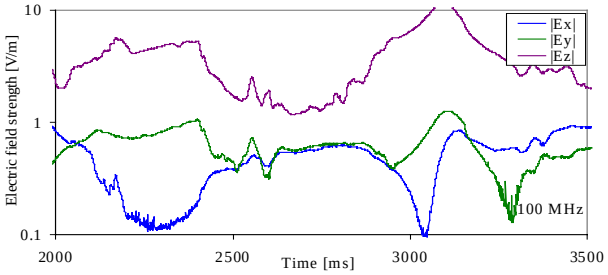

Figure 9: Stirring ratio at 100 MHz

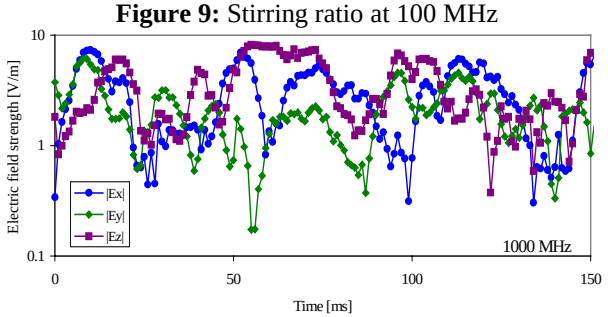

Figure 10: Stirring ratio at 1000 MHz

5.2. *Correlation coefficient (ρ)*

The three rectangular components of the electric field strength should be uncorrelated. The angular correlation coefficient is an indication for this figure. In Figure 11 the combined correlation coefficient is drawn as function of the frequency, according to:

$$\rho = \tfrac{1}{3}\left(\left|\rho_{xy}\right| + \left|\rho_{yz}\right| + \left|\rho_{yz}\right|\right)$$

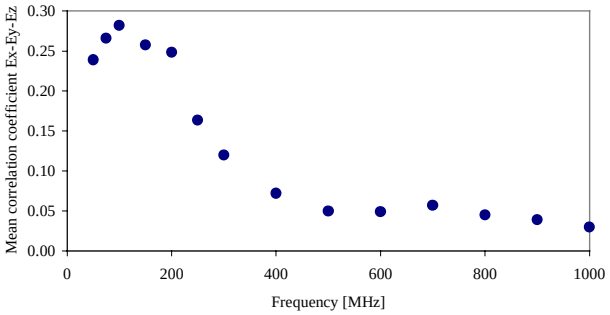

Figure 11: Combined correlation coefficient

A correlation coefficient ρ=1 implies that the signals are correlated. For instance, for ρ_{xy}=1, the field strength in *X*- and *Y*-direction would be equal. A ρ=0 indicates that the field strengths in the three directions are uncorrelated. Our objective for reverberation chambers is thus ρ=0 [7]. We can observe that already for relatively low frequencies the combined correlation coefficient is low.

5.3. *Probability density function*

To obtain the probability density function the measured absolute value of the electric field strengths in the three directions were normalized by their variance. Therefore the vectorial sum, denoted as E_{total}, is not a physic quantity anymore. The samples of this 'total electric field strength' have been sorted from the minimum field strength to the maximum field strength. This yields the experimental probability density function (PDF). By comparing the experimental PDF with the theoretical PDF, which should be X(6dof) [7], the quality of the chamber can be found: if the experimental PDF is equal to the theoretical PDF then the accuracy of a prediction is very high.

The procedure has been carried out for 6 measuring positions in a plane of 1.5x1.5 m, for the list of frequencies mentioned before. The PDFs are shown for the frequencies 100 MHz and 1 GHz in Figures 12 and 13. From these figures we can observe that at 100 MHz the PDF is not sufficiently smooth. Note that that this frequency is very low for a reverberation chamber of this dimension.

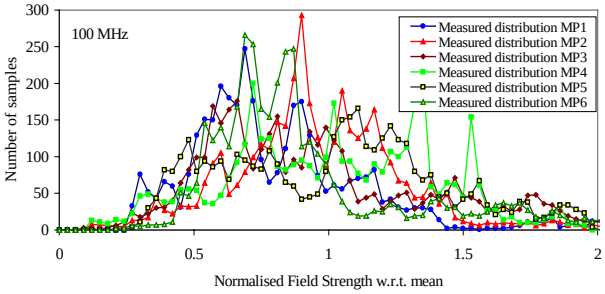

Figure 12: PDF for 6 measuring positions, 100 MHz

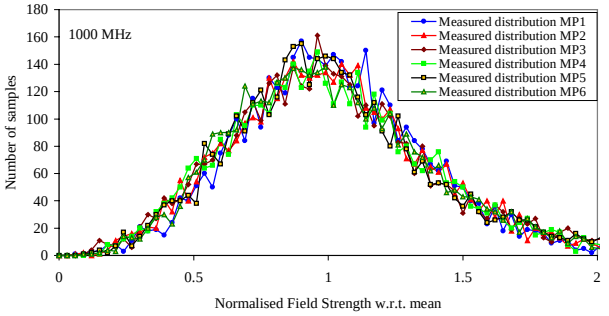

Figure 13: PDF for 6 measuring positions, 1000 MHz

At 1000 MHz the PDF is very smooth, and the curves for all 6 measuring positions are all within a very narrow band around the theoretical PDF.

5.4. *Cumulative density function*

The cumulative probability density function (CDF) is obtained by integrating the PDF. Via the CDF a comparison of PDFs for different frequencies or a comparison of chambers is facilitated. The CDFs are shown for the frequencies 100 MHz and 1 GHz in Figures 14 and 15 for all 6 measuring positions.

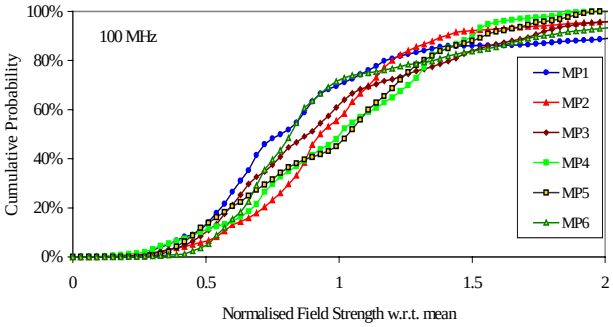

Figure 14: CDF for 6 measuring positions, 100 MHz

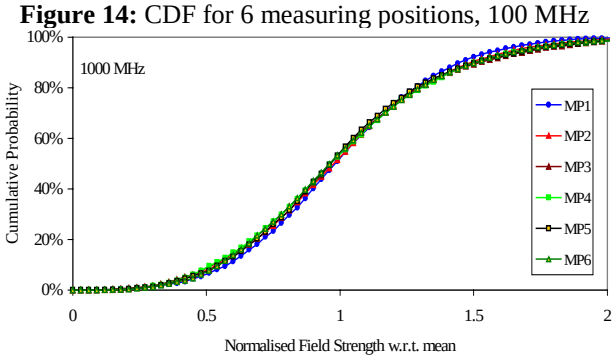

Figure 15: CDF for 6 measuring positions, 1000 MHz

5.5. *Spatial field uniformity*

Another important parameter is the spatial field uniformity (SFU). The SFU gives the ability to generate an isotropic, randomly polarised field, which is stochastic equal in the whole volume of the chamber, except near the walls. In Figure 16 the vectorial sum of the magnitude of the field strength in the three orthogonal directions, with respect to the mean field strength, per measuring position has been drawn as function of the frequency. From this figure we can conclude that the field strength is within the 0-6dB range for frequencies higher than 150 MHz.

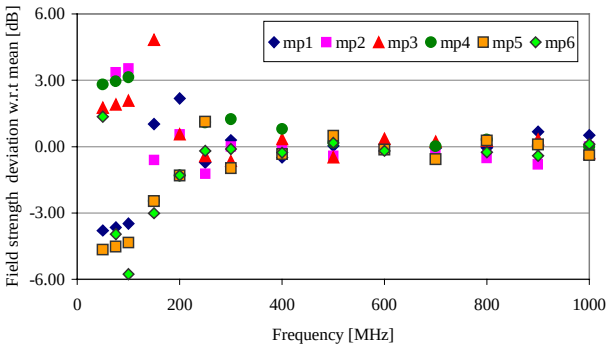

Figure 16: Field uniformity, 6 measuring positions

5.6. Chamber gain

The chamber gain (CG) gives us the average field strength increase with respect to a free space environment. In [7] the chamber gain is defined as

$$CG = \frac{16\pi^2 V}{\lambda^3 Q}$$

where V is the volume of the chamber and Q is the quality factor. The (loaded) quality factor is difficult to determine. Therefore a comparison measurement has been carried out in a full-anechoic chamber (free-space environment) and in the VIRC. The test set-up has been drawn in Figure 17.

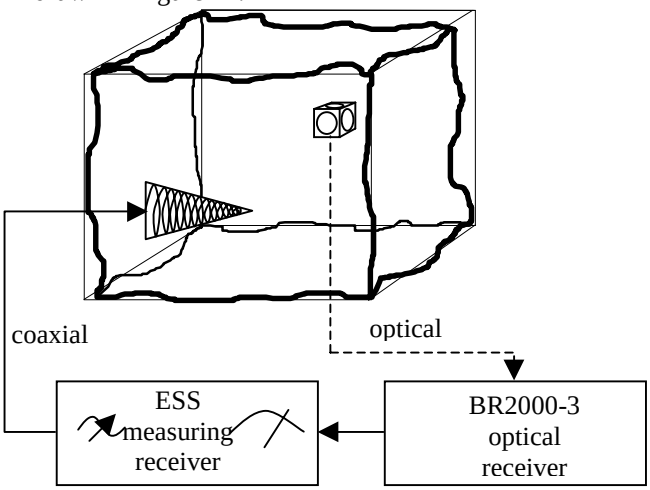

Figure 17: Test set-up for Chamber Gain measurement

An electromagnetic field was generated inside the VIRC by an antenna. The antenna was activated by the output of the tracking generator of the Rohde&Schwarz ESS measuring receiver. The field strength inside the VIRC has been measured using the Thomson-CSF ET2003 three-dimensional E-field sensor. The output signal of the sensor was fed to the optical receiver via an optical fiber. The output voltage level of the optical receiver was measured by the ESS measuring receiver for the three axes of the field. The received average field strength in free space environment and the VIRC have been compared. The difference is the chamber factor (CF), which is $CF = 20\log(CG)$. The CF has been drawn in Figure 17a for a linear frequency scale and figure 17b for a logarithmic frequency scale.

We can, again, observe a stable behaviour for frequencies higher than approximately 150 MHz. This is only 3 times the first resonance frequency.

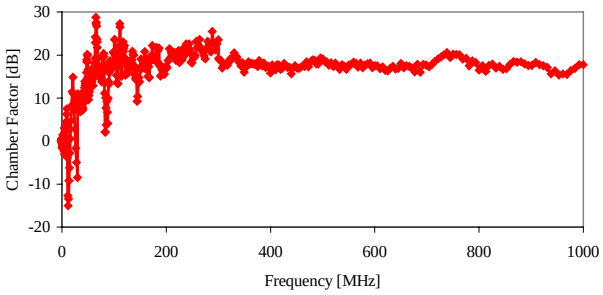

Figure 17a: Chamber factor, linear frequency scale

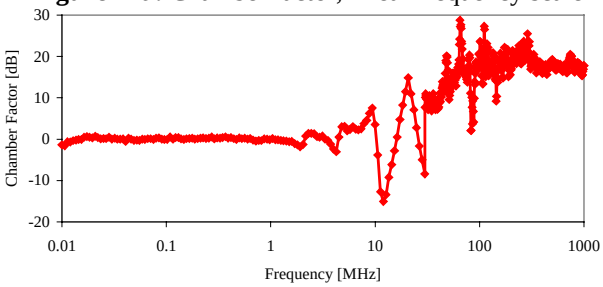

Figure 17b: Chamber factor, logarithmic scale

6. EMI measurements

The Equipment Under Test (EUT) is the multifunctional Active Phased Array Radar (APAR). A picture taken in front of the EUT is presented in Figure 18. The test set-up has been drawn schematically in Figure 19. Note that the EUT is part of the wall of the VIRC. Due to the fact that APAR is a classified product we can present only simplified data.

The VIRC was attached in front of the radar antenna making a galvanic connection over the whole circumference, as shown in Figure 6 and 7.

Radiated emission measurements and radiated immunity measurements have been performed and described shortly.

Figure 18: Test set-up: EUT in the VIRC, with an antenna placed in foreground

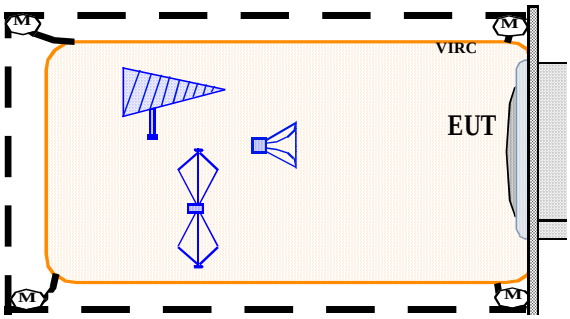

Figure 19: Test set-up

6.1. Radiated emission

The field strength has been measured as function of frequency. Average and peak detectors were used simultaneously. The measured field strength was corrected by means of the experimentally obtained Chamber Factor:

$$E = E_{measured} - CF$$

For frequencies below 10 MHz the CF equals 0. The radiated emission measurements performed in this frequency range therefore result in the same field strength as would be obtained in an anechoic chamber or free space environment. For frequencies above 10 MHz, the chamber factor is positively valued. Therefore the CF corrected field strength in the VIRC is much lower compared to the field strength which could have been measured in a free space environment!
Ambient measurements have been carried out to determine if the VIRC shielding effectiveness was retained. Only EMI receiver noise has been measured. This was also the case with the EUT activated. This means that the radiated emission was below the receiver noise upto 1 MHz, and even 20dB below receiver noise for frequencies higher than 10 MHz.

6.2. Radiated immunity

Inside the VIRC the maximum power, as available in our laboratories, was generated. This includes for instance 2500 W in the frequency band 10kHz-200MHz, 500 W 200 MHz- 1 GHz, and 200 W in the frequency band 1-18 GHz.
The generated field strength can be calculated via the chamber gain, or obtained via measurements. The measured maximum average field strength was beyond 1000 V/m, while the maximum peak field strength was nearly 10.000 V/m. The EUT did not show degradation of performance.

7. Conclusion

A new type of reverberation chamber to create a spatial uniform and isotropic electromagnetic field is the Vibrating Intrinsic Reverberation Chamber (VIRC). The major benefits of the VIRC are the extremely high field strength which can be generated for immunity testing. The increased dynamic range for emission testing is also beneficial, while the user-friendliness of the technique for in-situ testing has been shown.
A VIRC was designed for in-situ measurements on a multifunctional active phased array radar. The VIRC has been validated prior to the use on the equipment under test. The test results show that the VIRC fulfils the de-facto requirements on reverberation chamber testing for a large frequency range. The EMI measurements could therefore be carried out with a high confidence level.

References

[1] H.A. Mendes, A New Approach to Electromagnetic Field Strength Measurements in Shielded Enclosures, Wescon Technical Papers, Western Electronic Show and Convention, Aug. 20-23, 1968, Los Angeles.
[2] P. Corona, G. Latmiral, E. Paolini, L. Piccioli, Use of a reverberating enclosure for measurements of radiated power in the microwave range, IEEE Transactions on Electromagnetic Compatibility, May 1976, p.54-59.
[3] M.L. Crawford, G.H. Koepke, Operational Considerations of a Reverberation Chamber for EMC immunity Measurements - Some Experimental Results, IEEE Symposium on EMC, 1984.
[4] M.L. Crawford, G.H. Koepke, Design, Evaluation and Use of a Reverberation Chamber for Performing Electromagnetic Susceptibility/ Vulnerability Measurements, NBS Nt 1092, 1986.
[5] F.B.J. Leferink, J.C. Boudenot, W. van Etten, The Vibrating Intrinsic Reverberation Chamber: an Optimal Use of Geometrical Change in Boundary Conditions, Report University of Twente, EL-TEL, sept. 1999.
[6] Y. Huang, Conducting triangular chambers for EMC measurements, Meas.Sci.Technol, 10, 1999, L21-L24
[7] D.A. Hill, Electromagnetic theory of reverberation chambers, NIST Technical note 1506, dec. 1998.
[8] J.M. Dunn, Local, High-Frequency Analysis of the Fields in a Mode-Stirred Chamber, IEEE Transactions on Electromagnetic Compatibility, Febr. 1990, pp. 53-58.
[9] F.B.J. Leferink, High field strength in a large volume: the intrinsic reverberation chamber, IEEE Symposium on EMC, 1998, pp. 25-27.
[10] A.C. Marvin, J.A.S. Angus, J.F. Dawson, J. Clegg, 'Enhancements to Stirred Mode Chambers by the Use of Pseudo-Random Phase reflection Gratings', Int. Symposium on EMC, Rome, Italy, 1994, pp. 218-221.
[11] J. Clegg, A.C. Marvin, J.A.S. Angus, J.F. Dawson, 'Optimal Phase Reflection gratings and the Effect on Fields in a Mode Stirred Chamber', Int. Symposium on EMC, Rome, Italy, 1996.
[12] M. Petirsch, A. Schwab, 'Optimizing Shielded Chambers Utilizing Acoustic Analogies', IEEE Symposium on EMC, 1997, pp. 154-158.
[13] E.A. Godfrey, Effects of corrugated walls on the field uniformity of reverberation chambers at low frequencies, IEEE Symposium on EMC, 1999, pp. 23-28.
[14] Y. Huang, D.J. Edwards, An investigation of electromagnetic fields inside a moving wall mode-stirred chamber, IEE Conference on EMC, Edinburgh, 1992.
[15] M. Hatfield, Visualisation of Electromagnetis Fields in a Rev. Chamber, Experiments Session IEEE EMC Symposium 1998.
[16] F.B.J. Leferink, W.C. van Etten, The Vibrating Intrinsic Reverberation Chamber, IEEE Tr. on EMC, 2001.
[17] F.B.J. Leferink, J.C. Boudenot, W.C. van Etten, Experimental Results Obtained in the Vibrating Intrinsic Reverberation Chamber, IEEE Symposium on EMC, Washington D.C. 2000.
[18] F.B.J. Leferink, W.C. van Etten, Optimal Utilization of a Reverberation Chamber, 4th European Symposium on Electromagnetic Compatibility, Brugge, 2000.
[19] Patent WO34795, NL1010745, AU18605 etc, Test Chamber, Hollandse Signaalapparaten B.V., Netherlands.